Linear Viscoelastic Moduli of Concentrated DNA Solutions

T. G. Mason,* A. Dhople, and D. Wirtz

Department of Chemical Engineering, Johns Hopkins University, 221 Maryland Hall, 3400 North Charles Street, Baltimore, Maryland 21218

ABSTRACT: We present mechanical measurements of the frequency-dependent linear viscoelastic storage and loss moduli, $G'(\omega)$ and $G''(\omega)$, for calf thymus DNA (13 kbp) in a saline buffer over a range of mitotically relevant mass concentrations from $C = 1$ to 10 mg/mL. For C exceeding a critical entanglement concentration, C_e, we observe a dominant plateau elasticity, G'_p, for large ω. As ω decreases, G' falls until it is equal to G'' at the crossover frequency, ω_c, below which G'' dominates. These measurements are consistent with a model of entangled semiflexible polymer coils in a good solvent, which predicts $G'_p \sim C^{2.3}$ and $\omega_c \sim C^{-2.4}$.

1. Introduction

Deoxyribonucleic acids (DNA) are important biopolymers that contain genetic information and are found in many living cells. Depending upon the type of cell and the stage in its life cycle, DNA may be present in a variety of different forms. One of the most prevalent is linear, double-stranded DNA consisting of a charged, double-helical scaffolding between which complimentary nucleotides are bound;[1] this double-helix provides both bending and twist rigidity,[2,3] making linear DNA a semiflexible, charged polymer chain. During the prometaphase stage of mitosis, DNA is concentrated within the nuclei of cells before replication and separation occur. In a typical mammalian cell, 10^9 nucleotides occupy a volume of 100 μm^3,[1] yielding a DNA mass concentration of $C \approx 10$ mg/mL. At such high concentrations, DNA molecules having contour lengths of several microns can become entangled. This may lead to an elastic rheological response to an applied shear typical of polymers in their semidilute regime.[4] In cell division, this entanglement elasticity could prevent the separation of the DNA after replication through the contraction of microtubules connected to the mitotic spindles. However, the action of an ATP-powered enzyme, known as Topoisomerase II (Topo II), which transiently cuts and rebonds one of two crossed DNA at an entanglement site,[5] has been hypothesized as the mechanism through which the entanglements relax and the chromosomes are separated. Before addressing how Topo II may alter the viscoelastic relaxation of entangled DNA,[6,7] it is first necessary to understand the viscoelasticity of DNA at high concentrations in the absence of the enzyme.

A previous investigation of the shear rheology of DNA solutions extracted the longest retardation time, τ_R, and viscosity, η, from creep recovery experiments of dilute T2 and T7 bacteriophage DNA in BBES and glycerol buffers for the purposes of identifying their average molecular weight.[8] At much larger concentrations of T2 DNA in a saline buffer, τ_R and η have been measured in the entanglement regime using a magnetic ball rheometer;[4] the characteristic plateau elasticity has been extracted from these values but not directly measured. This experiment supports the hypothesis that the critical concentration, C_e, at which the DNA begin to become entangled is greater than the critical overlap concentration,[9] C^*, of DNA coils.

In contrast to these methods, we have used a controlled strain rheometer to measure the strain and frequency dependencies of the elastic storage modulus, G', and dissipative loss modulus, G'', of concentrated linear calf thymus DNA in a saline buffer, which could support the activity of Topo II. We explore DNA concentrations up to 10 mg/mL, well into the entanglement regime. For small strains corresponding to a linear viscoelastic rheological response, our measurements reveal the onset of a dominant plateau in $G'(\omega)$ with increasing C at the highest ω we probe; this plateau modulus, G'_p, reflects the entanglement elasticity. At lower ω, the storage modulus falls until it equals the loss modulus at the crossover frequency, ω_c, below which the loss modulus dominates, reflecting the relaxation of the entanglements. Both G'_p and ω_c scale with C according to classical predictions for polymer entanglement networks. Moreover, a simple model of the elasticity is in good agreement with the measured magnitude of G'_p.

2. Experiment

Large volumes of DNA solution are required for performing standard mechanical rheometry, so we have chosen purified sodium DNA from calf thymus, which is available in sufficient quantity. These linear, double-stranded DNA are fragments of longer chromosomes and have a weight-average molecular weight of $N = 1.3 \times 10^4$ base pairs (bp). We disperse the dehydrated DNA in an aqueous buffer containing [Tris−HCl] (pH 7.9) = 10 mM, [NaCl] = 50 mM, [KCl] = 50 mM, [MgCl$_2$] = 5 mM, [BSA] = 15 μg/mL, and [EDTA] = 0.1 mM. (Residual sodium present on the dehydrated DNA leads to a slightly larger [Na$^+$] = 60 mM when dispersed.) We have chosen this saline buffer because it can support the activity of enzymes such as Topo II. Phenol−chloroform extraction has been used to eliminate contaminating proteins. An optically homogeneous solution at $C = 10$ mg/mL is attained through gentle mechanical agitation over 5 days. Lower C have been reached by diluting this concentrated stock solution and allowing equilibration over 1 day. To inhibit degradation, the DNA solutions have been stored in a refrigerator at $T = 4$ °C after mixing. All measurements have been made within 1 week after the DNA have been added to the buffer at $T = 25$ °C.

* Corresponding author. Present address: Exxon Research & Engineering Co., Route 22 East, Annandale, NJ 08801.
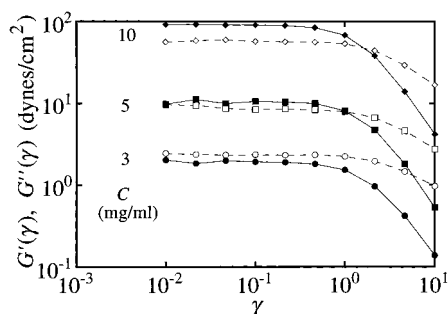
Figure 1. Strain dependence of the storage modulus, G' (solid symbols), and the loss modulus, G'' (open symbols), for calf thymus DNA concentrations of $C = 3$ mg/mL (circles), 5 mg/mL (squares), and 10 mg/mL (diamonds). The frequency is fixed at $\omega = 1$ rad/s.
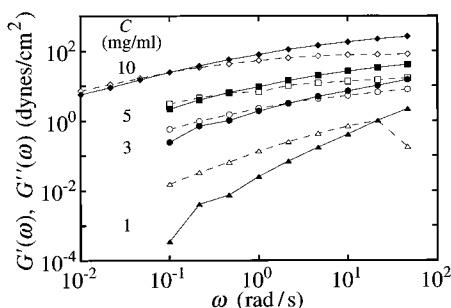

Figure 2. Frequency dependence of the storage modulus, G' (solid symbols), and the loss modulus, G'' (open symbols), for DNA concentrations of $C = 1$ mg/mL (triangles), 3 mg/mL (circles), 5 mg/mL (squares), and 10 mg/mL (diamonds). The strain amplitude is fixed at $\gamma = 0.02$.

To measure the frequency dependencies of the storage and loss moduli, we employ a controlled strain mechanical rheometer equipped with a 25 mm diameter cone (angle 0.1 rad) and plate geometry requiring a sample volume of about 200 μL. We have chosen this geometry because it produces a uniform strain field, so that a unique strain amplitude, γ, can be used to define the deformation. The highest frequency we can reliably probe is $\omega = 46$ rad/s, limited by the mechanical inertia of the rheometer tools. For all C and ω we explore, the shear wavelength significantly exceeds the maximum gap at the edge of the cone, so all measurements are made in the gap loading limit.[10] Evaporation of the water at the exposed surface between the cone and plate can lead to an anomalous increase in the measured elasticity over time; a vapor trap has been employed to eliminate this artifact.

3. Results

To measure the linear viscoelastic moduli, we locate the strain regime in which G' and G'' are independent of γ. We set $\omega = 1$ rad/s and sweep γ from low to high. For strains less than the yield strain of $\gamma_y \approx 0.7$, we find that G' and G'' are independent of γ for all C, as shown in Figure 1. Similar measurements at higher and lower ω do not reveal any decrease in the yield strain, so any fixed strain below γ_y will yield linear moduli for all frequencies we probe.

By fixing $\gamma = 0.02$, well within the linear regime, and sweeping ω from low to high, we measure the spectra for the storage and loss moduli for different DNA concentrations. The results are plotted in log−log format in Figure 2. At the highest $C = 10$ mg/mL, a plateau in G' is evident at high ω where G' dominates G'' and has a slope approaching zero. Moving toward lower ω, a dropoff in the plateau is observed, and G'' begins to dominate G' below the crossover frequency, ω_c. These general spectral features can be seen for

smaller $C = 5$ mg/mL and $C = 3$ mg/mL, albeit with weaker plateau elasticities and higher crossover frequencies. However, at $C = 1$ mg/mL, G' at the lowest frequencies is much smaller than G'', and it is nearly 3 orders of magnitude smaller than G' at $C = 3$ mg/mL, a much larger relative decrease in the low-frequency G' than the 1 order of magnitude drop observed from $C = 5$ to 3 mg/mL. Moreover, at $C = 1$ mg/mL, the loss modulus dominates over nearly the whole range of ω we probe and depends linearly on ω at low frequencies, reflecting a viscosity about 10 times that of water.

4. Analysis

To understand the concentration dependence of the viscoelastic moduli, we apply the standard model of entangled flexible polymer solutions[9] to the DNA solution. We assume that the DNA chains in solution form coils that can be imagined as a random walk of rigid segments having Kuhn lengths equal to twice the bending persistence length, L_p, which is proportional to the local bending modulus of the DNA chain.[11] When the concentration of the coils is raised so that they pack and entangle in disordered configuration, a dominant elastic modulus that is entropic in origin develops. Provided the contour length of the DNA is much larger than the persistence length, the scaling laws for the concentration and frequency dependencies of the viscoelastic moduli that are known for flexible polymer solutions should also apply to semiflexible polymer solutions.

The radius of gyration of a semiflexible polymer coil is given by[11]

$$R_g = 2L_p(N_p/6)^\nu \qquad (1)$$

where $N_p = aN/(2L_p)$ is the effective number of Kuhn segments, $a = 3.4$ Å is the length of a base pair, and $\nu = 0.59$ for a good solvent corresponding to a self-avoiding random walk whereas $\nu = 0.5$ for a Θ-solvent corresponding to an ideal random walk. Equation 1 is an approximation for chains that have a total contour length much greater than L_p, i.e., $N_p \gg 1$. The explicit dependence of R_g on L_p can be obtained by substituting for N_p:

$$R_g = 2L_p(aN/12L_p)^\nu \qquad (2)$$

For fixed persistence and contour lengths, the coils of rigid segments in a Θ-solvent are smaller than those for a good solvent.

When the concentration of coils is raised so that they begin to overlap and entangle, a dominant plateau elastic shear modulus can develop. This concentration has been traditionally assigned to be the mass density of monomers in a single coil and is known as the critical overlap concentration, C^*:[9]

$$C^* \approx \rho N/R_g^3 \qquad (3)$$

where $\rho = 1.1 \times 10^{-21}$ g/bp is the linear mass per base pair. This estimate neglects constant factors, but it has been used to define the "semidilute" regime for $C > C^*$. However, C^* may not define the true entanglement concentration, C_e, at which the onset of the plateau elastic modulus is observed. Recent experiments with synthetic polymers in good solvents[12] suggest that an overlap does not correspond directly to an entanglement
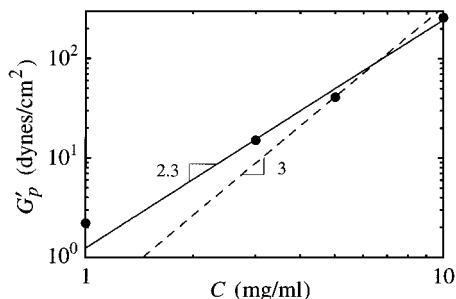
Figure 3. Dependence of the plateau storage modulus, G'_p, on DNA concentration, C. The solid line is a fit to the scaling predicted for a good solvent, yielding $G'_p = 6.1\ (C/C_e)^{2.3}$ dynes/cm², and the dashed line is a fit to the scaling predicted for a Θ-solvent, yielding $G'_p = 2.7\ (C/C_e)^3$ dynes/cm².

that can store shear energy. Instead, C_e can be considerably larger than the overlap concentration: $C_e \approx C^* N_e^{3\nu-1}$, where N_e represents the average number of monomers along the chain between entanglement points.

On the basis of the observed onset of the elastic plateau between $C = 1$ mg/mL and $C = 3$ mg/mL in Figure 2, we conclude that the critical entanglement concentration is $C_e \approx 2$ mg/mL. From this value and the predicted C^* calculated using a reported value of L_p, we determine N_e by assuming either a good solvent or a Θ-solvent. For Col E₁ DNA (6.6 kbp) in a saline solution similar to ours, L_p has been determined from angle- and concentration-dependent light-scattering measurements.[13,14] At the ionic strength of our buffer, $L_p \approx 500$ Å ≈ 147 bp. This L_p is consistent with other measurements using a variety of methods.[15] For calf thymus DNA, this persistence length implies there are $N_p = 44$ Kuhn segments. Using eq 1 we find $R_g = 324$ nm and $C^* = 0.35$ mg/mL for a good solvent whereas $R_g = 271$ nm and $C^* = 0.7$ mg/mL for a Θ-solvent. This implies that there are $N_e \approx 10$ Kuhn segments between entanglement points for a good solvent whereas $N_e \approx 8$ segments for a Θ-solvent.

At frequencies above those corresponding to the relaxation of entanglements, the concentrated DNA solution can store shear energy. Above C_e, the scaling of G'_p with C has also been predicted by decomposing the coil into blobs: $G'_p \sim C^{3\nu/(3\nu-1)}$.[12,16] This scaling form can be conveniently rewritten as:

$$G'_p(C) = G'_p(C_e)[C/C_e]^{3\nu/(3\nu-1)} \qquad (4)$$

where $G'_p(C_e) = k_B T C_e/(\rho N) = k_B T N_e^{3\nu-1}/R_g^3$ is the plateau modulus at the entanglement concentration and k_B is Boltzmann's constant. Since the scaling exponent depends on ν, a measurement of $G'_p(C)$ should determine the effective solvent condition. We extract $G'_p(C)$ from the storage moduli shown in Figure 2. In principle, if $G'(\omega)$ is known over an arbitrarily large range of ω, then the plateau modulus, G'_p, can be precisely defined as the value of G' at the inflection point in $G'(\omega)$. However, the data for $G'(\omega)$ do not extend to large enough frequencies for the inflection point to be seen, so we instead define G'_p to be the value of $G'(\omega)$ at $\omega = 46$ rad/s, as far above the crossover frequency as we are able to measure. We plot $G'_p(C)$ as the solid circles in Figure 3. By fitting the observed rise using eq 4 with $C_e = 2$ mg/mL, we find better agreement for a good solvent (solid line of slope 2.3) with $G'_p(C_e) = 6.1 \pm 3.1$ dynes/cm² than for a Θ-solvent (dashed line of slope 3) with $G'_p(C_e) = 2.7 \pm 1.5$ dynes/cm². The value
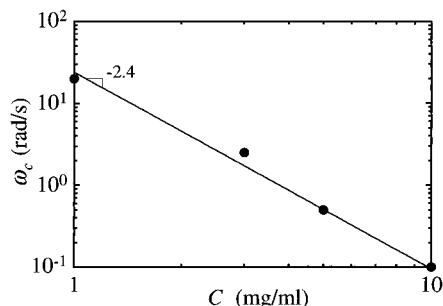

Figure 4. Dependence of the crossover frequency, ω_c, on DNA concentration, C. The solid line is a fit to the semiempirical scaling, yielding $\omega_c = 4.5(C/C_e)^{-2.4}$ rad/s.

of $G'_p(C_e)$ from the fit for the good solvent is also in accord with the thermal estimate $G'_p(C_e) = 6.9$ dynes/cm² calculated using $R_g = 324$ nm and $N_e = 10$.

At very low frequencies, the entanglements of the polymer solution are able to relax; this relaxation can be characterized by a low-frequency viscosity, η, which can be related to the crossover frequency, ω_c, where the elastic storage modulus equals the viscous loss modulus: $G'(\omega) = G''(\omega)$. From the measured spectra in Figure 2, we directly obtain ω_c and plot it as a function of C in Figure 4. An estimate for the concentration dependence of ω_c can be made by equating the viscous loss modulus with the plateau storage modulus $\eta\omega_c = G'_p$. Synthetic flexible polymers in a good solvent are known to follow the empirical relationships, $G'_p \sim C^{2.3}$ and $\eta \sim C^{4.7}$,[12] implying that the crossover frequency scales as $\omega_c \sim C^{-2.4}$. This scaling form compares well with the data for ω_c, as shown by the solid line in Figure 4, and we find $\omega_c = 4.5 \pm 2.3(C/C_e)^{-2.4}$ rad/s. From ω_c and G'_p for a good solvent, we may infer that the low-frequency viscosity is $\eta = G'_p/\omega_c = 1.4\ (C/C_e)^{4.7}$ P. By comparing this with a reported empirical form: $\eta = 60\eta_s(C[\eta])^{1.3}(C/C_e)^{3.4}$,[12] where $[\eta]$ is the intrinsic viscosity of the DNA and η_s is the solvent viscosity (which for water is $\eta_s = 1$ cP), we extract the intrinsic viscosity of the calf thymus DNA: $[\eta] = 1$ cm³/mg. Since the intrinsic viscosity is expected to be inversely proportional to the critical concentration, this result is in reasonable agreement with the larger $[\eta] = 30$ cm³/mg[17] for longer T2 DNA, which have a lower entanglement concentration $C_e = 0.25$ mg/mL.[4]

5. Discussion

Our direct measurements of the concentration dependence of the plateau elasticity and crossover frequency are in good agreement with predictions of $G'_p(C) \sim C^{2.3}$ and $\omega_c(C) \sim C^{-2.4}$ based on a model of semiflexible polymer coils in a good solvent. The relatively poor agreement of the ideal Θ-solvent scaling, $G'_p(C) \sim C^3$, with the data suggests that the excluded volume of the segments is important and cannot be neglected. Moreover, since $N_p \approx 44$ is sufficiently large, it is reasonable to model the DNA as a coil composed of segments characterized by a Kuhn length that is considerably smaller than R_g. The measured values of $C_e = 2$ mg/mL and $G'_p(C_e) = 6.1$ dynes/cm² for calf thymus DNA are consistent with $L_p \approx 500$ Å, provided there are $N_e = 10$ segments between entanglements. While this value is small compared to $N_e \approx 100$ for flexible polymers in good solvents,[12] it is reasonable since we would not expect $N_e > N_p$. Having a theoretical prediction of N_e for semiflexible polymers as a function of N_p

would be useful for comparison, but we know of no such prediction.

Our analysis has focused primarily on interpreting the concentration dependence of the gross features of the measured viscoelastic spectra. However, understanding the precise shapes of $G'(\omega)$ and $G''(\omega)$ at a given C would provide additional microscopic insight into the relaxation mechanisms of semiflexible entanglement networks. For all concentrations we have measured, the spectra cannot be systematically fit using the standard reptation model for monodisperse flexible polymers.[18] The inability of the reptation model to predict the measured spectra of synthetic flexible polymers is well-established, so its failure to describe our measurements of the DNA spectra is not surprising.

Since we clearly observe a dominant $G''(\omega)$ at low frequencies, we deduce that DNA coils at this ionic strength are not strongly attractive and do form a gel having a dominant zero-frequency elasticity. The absence of strong intercoil attractions implied by this result is presumably due to the electrostatic screening by the ions in solution. Since DNA have ionic sites, their rheological properties may differ from those of uncharged synthetic polymers. Our measurements indicate that this is not the case for the saline buffer we have used; the scaling laws for the plateau elasticity and crossover frequency of entangled linear DNA are consistent with those predicted generically for coils composed of rigid segments in a good solvent just above the entanglement concentration.[16] This result is in agreement with the general finding that screened polyelectrolytes essentially behave like uncharged polymers in good solvents.[19] However, this does not rule out the possibility that the viscoelastic spectra of DNA may be different than we have observed at significantly lower ionic strengths.

Our experiments also show that aging effects can play a significant role in DNA rheology. Particle tracking microrheology measurements of the viscoelastic moduli have been made for concentrated DNA at $C = 10$ mg/mL after 1 month of aging;[20] since degradation due to aging has been found in early DNA rheology experiments (e.g., ref 21), it is not surprising that the moduli we present here for freshly purified DNA differ.

The measured yield strain of $\gamma_y \approx 0.7$ above C_e implies that nonlinear rheological behavior arises only after the shear causes one coil to be translated relative to a neighboring coil by a distance of the coil radius. This yield strain is similar to that seen for flexible polymers.[22] However, it is large compared to those of other disordered colloids, such as compressed emulsions and hard sphere glasses, which can have $\gamma_y < 0.01$.[23,24] The large value of γ_y for DNA implies that the entanglements strongly inhibit the development of microscopic shear-induced slippage between coils.

Real chromosomes inside nuclei are organized at many length scales.[1] The disordered, isotropic solution of reconstituted DNA fragments we have used in this investigation has a much different structure. Although our observations may not reflect the organized structures of real chromosomes during mitosis, they do show that the elasticity of entangled DNA could inhibit mitosis in the absence of enzymes that actively relax entanglements such as Topo II. Thus, our measurements set the stage for rheological investigations of entangled DNA in the presence of Topo II.

6. Conclusion

The direct observations of the frequency dependencies of the storage and loss moduli support the hypothesis that concentrated DNA in a saline buffer behave as an entanglement network of semiflexible coils in a good solvent, exhibiting an elastic modulus and a crossover frequency that vary with concentration according to known scaling laws. Both the measured entanglement concentration associated with the sharp rise in $G'(\omega)$ at low ω and the magnitude of the plateau modulus are in good quantitative agreement with this model. Moreover, they are also consistent with reported values of the persistence length of DNA at the ionic strength we have used. We anticipate that these results will serve as a basis for comparison with future experiments in which Topo II and ATP are added to the concentrated DNA solution to actively relax entanglements.

References and Notes

(1) Alberts, B.; Bray, D.; Lewis, J.; Raff, M.; Roberts, K.; Watson, J. D. *Molecular Biology of the Cell*; Garland: New York, 1990.
(2) Manning, G. S. *Biopolymers* **1988**, *27*, 1529.
(3) Marko, J. F. *Phys. Rev. E* **1997**, *55*, 1758.
(4) Musti, R.; Sikorav, J.-L.; Lairez, D.; Jannink, G.; Adam, M. *C. R. Acad. Sci. II* **1995**, *320*, 599.
(5) Holm, C. *Cell* **1994**, *77*, 955.
(6) Sikorav, J.-L.; Jannink, G. *C. R. Acad. Sci. II* **1993**, *316*, 751.
(7) Sikorav, J.-L.; Jannink, G. *Biophys. J.* **1994**, *66*, 827.
(8) Klotz, L. C.; Zimm, B. H. *J. Mol. Biol.* **1972**, *72*, 779.
(9) deGennes, P.-G. *Scaling Concepts in Polymer Physics*; Cornell University Press: Ithaca, NY, 1979.
(10) Schrag, J. L. *Trans. Soc. Rheol.* **1977**, *21*, 399.
(11) Doi, M.; Edwards, S. F. *The Theory of Polymer Dynamics*; Oxford University Press: Oxford, U.K., 1986.
(12) Raspaud, E.; Lairez, D.; Adam, M. *Macromolecules* **1995**, *28*, 927.
(13) Manning, G. S. *Biopolymers* **1981**, *20*, 1751.
(14) Borochov, N.; Eisenberg, H.; Kam, Z. *Biopolymers* **1981**, *20*, 231.
(15) Porschke, D. *Biophys. Chem.* **1991**, *40*, 169.
(16) Morse, D. C. *Macromolecules*, submitted.
(17) Chapman, R. E.; Klotz, L. C.; Thompson, D. S.; Zimm, B. H. *Macromolecules* **1969**, *2*, 637.
(18) deGennes, P. G. *J. Chem. Phys.* **1971**, *55*, 572.
(19) Pfeuty, P. *J. Phys.* **1978**, *39*, C2−149.
(20) Mason, T. G.; Ganesan, K.; van Zanten, J. H.; Wirtz, D.; Kuo, S. C. *Phys. Rev. Lett.* **1997**, *79*, 3282.
(21) Helders, F. E.; Ferry, J. D.; Markovitz, H.; Zapas, L. J. *J. Phys. Chem.* **1956**, *60*, 1575.
(22) Osaki, K.; Nishizawa, K.; Kurata, M. *Macromolecules* **1982**, *15*, 1068.
(23) Mason, T. G.; Bibette, J.; Weitz, D. A. *Phys. Rev. Lett.* **1995**, *75*, 2051.
(24) Mason, T. G.; Weitz, D. A. *Phys. Rev. Lett.* **1995**, *75*, 2770.